Article

Surface Chemistry of Colloidal PbSe Nanocrystals

Iwan Moreels, Bernd Fritzinger, Jose# C. Martins, and Zeger Hens

J. Am. Chem. Soc., **2008**, 130 (45), 15081-15086 • DOI: 10.1021/ja803994m • Publication Date (Web): 17 October 2008

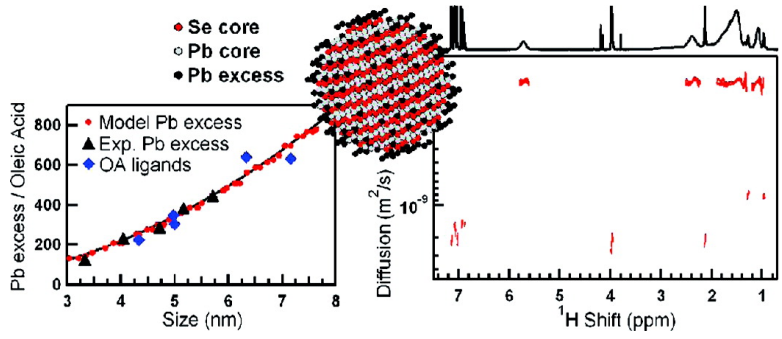

More About This Article

Additional resources and features associated with this article are available within the HTML version:

- Supporting Information
- Access to high resolution figures
- Links to articles and content related to this article
- Copyright permission to reproduce figures and/or text from this article

View the Full Text HTML

J|A|C|S
ARTICLES

Published on Web 10/17/2008

Surface Chemistry of Colloidal PbSe Nanocrystals

Iwan Moreels,[†] Bernd Fritzinger,[‡] José C. Martins,[‡] and Zeger Hens*,[†]

Physics and Chemistry of Nanostructures, Ghent University, Krijgslaan 281-S12, BE-9000 Ghent, Belgium, and NMR and Structure Analysis Unit, Ghent University, Krijgslaan 281-S4bis, BE-9000 Ghent, Belgium

Received May 28, 2008; E-mail: Zeger.Hens@UGent.be

Abstract: Solution nuclear magnetic resonance spectroscopy (NMR) is used to identify and quantify the organic capping of colloidal PbSe nanocrystals (Q-PbSe). We find that the capping consists primarily of tightly bound oleic acid ligands. Only a minor part of the ligand shell (0−5% with respect to the number of oleic acid ligands) is composed of tri-*n*-octylphosphine. As a result, tuning of the Q-PbSe size during synthesis is achieved by varying the oleic acid concentration. By combining the NMR results with inductively coupled plasma mass spectrometry, a complete Q-PbSe structural model of semiconductor core and organic ligands is constructed. The nanocrystals are nonstoichiometric, with a surface that is composed of lead atoms. The absence of surface selenium atoms is in accordance with an oleic acid ligand shell. NMR results on a Q-PbSe suspension, stored under ambient conditions, suggest that oxidation leads to the loss of oleic acid ligands and surface Pb atoms, forming dissolved lead oleate.

1. Introduction

Over the last 10 years, lead selenide colloidal quantum dots (Q-PbSe) have become a prominent example of the advantages that nanocrystalline material can offer. Bulk PbSe has a band gap of only 0.28 eV at room temperature, and the bulk exciton Bohr radius (46 nm) is among the largest for semiconductor materials. Consequently, small (2−10 nm) PbSe nanocrystals show extreme quantum confinement and their band gap can be tuned over the entire near-infrared wavelength region (1−4 μm).[1,2] Since the development of a nearly perfect synthesis route for colloidal Q-PbSe based on lead oleate [$Pb(OA)_2$] and tri-*n*-octylphosphine selenide (TOPSe), referred to as the Murray synthesis[1] hereafter, several groups have shown that these nanocrystals possess extraordinary optical properties, such as a high photoluminescence efficiency,[3] efficient multiple exciton generation,[4] and a high nonlinear refractive index.[5] Not surprisingly, it has become the material of choice for a wide range of potential applications, including Q-dot lasers operating at telecom wavelengths,[6] solar cells,[7] and even applications in the field of nonlinear optics.[8,9]

PbSe nanocrystals, like most colloidal nanocrystals, come with a capping of organic ligands, and the chemistry of this organic|inorganic interface strongly affects their physical and chemical properties. Recently, interest in this intimate interplay between the ligands and the nanocrystal surface has grown considerably. It was shown for instance that, by limiting the growth rate of specific lattice planes during synthesis, the ligands determine the size and shape of the nanocrystals, leading to the growth of quantum rods, wires, or tetrapods.[10] In addition, the ligands ensure colloid stability by steric hindrance, and the type of ligands (hydrophobic vs hydrophilic) determines the nanocrystal solubility.[11] They also passivate surface states, yielding nanocrystals with a high photoluminescence,[3] and the ligand chain length determines the electrical conductivity of quantum dot solids.[12] These examples make it clear that the ligands play an essential role in the nanocrystal synthesis and processing.

At present, a major problem hampering the routine chemical investigation of this organic|inorganic interface is the lack of well-established methods to identify and quantify the nanocrystal ligands and the corresponding ligand dynamics.[10] As a result, the role of the ligands and the effect of ligand engineering have only been demonstrated by indirect means in the cases mentioned above, by for instance a change in solubility after capping exchange, or an increase in the conductivity after treatment with a short chain ligand. Recently, several experimental studies on sterically stabilized colloidal nanoparticles have shown that nuclear magnetic resonance spectroscopy (NMR) holds considerable promise for the in situ characterization of the organic ligands. Ligand identification has been demonstrated in the case

[†] Physics and Chemistry of Nanostructures.
[‡] NMR and Structure Analysis Unit.

(1) Murray, C. B.; Sun, S. H.; Gaschler, W.; Doyle, H.; Betley, T. A.; Kagan, C. R. *IBM J. Res. Dev.* **2001**, *45*, 47.
(2) Pietryga, J. M.; Schaller, R. D.; Werder, D.; Stewart, M. H.; Klimov, V. I.; Hollingsworth, J. A. *J. Am. Chem. Soc.* **2004**, *126*, 11752.
(3) Du, H.; Chen, C. L.; Krishnan, R.; Krauss, T. D.; Harbold, J. M.; Wise, F. W.; Thomas, M. G.; Silcox, J. *Nano Lett.* **2002**, *2*, 1321.
(4) Schaller, R. D.; Klimov, V. I. *Phys. Rev. Lett.* **2004**, *92*, 186601.
(5) Moreels, I.; Hens, Z.; Kockaert, P.; Loicq, J.; Van Thourhout, D. *Appl. Phys. Lett.* **2006**, *89*, 193106.
(6) Schaller, R. D.; Petruska, M. A.; Klimov, V. I. *J. Phys. Chem. B* **2003**, *107*, 13765.
(7) Qi, D. F.; Fischbein, M.; Drndic, M.; Selmic, S. *Appl. Phys. Lett.* **2005**, *86*, 093103.
(8) Haurylau, M.; Zhang, J.; Weiss, S. M.; Fauchet, P. M.; Martyshkin, D. V.; Rupasov, V. I.; Krivoshlykov, S. G. *J. Photochem. Photobiol. A-Chem.* **2006**, *183*, 329.
(9) Brumer, M.; Sirota, M.; Kigel, A.; Sashchiuk, A.; Galun, E.; Burshtein, Z.; Lifshitz, E. *Appl. Opt.* **2006**, *45*, 7488.
(10) Yin, Y.; Alivisatos, A. P. *Nature* **2005**, *437*, 664.
(11) Yu, W. W.; Falkner, J. C.; Shih, B. S.; Colvin, V. L. *Chem. Mater.* **2004**, *16*, 3318.
(12) Talapin, D. V.; Murray, C. B. *Science* **2005**, *310*, 86.

of thiol- and TOP-TOPO-capped CdSe,[13,14] thiophenol-capped CdS,[15] lauric acid-capped CeO_2,[16] acetylacetonate-capped TiO_2,[17] and TOPO-capped InP nanocrystals.[18,19] For the last system, adsorbed TOPO was distinguished from residual unbound TOPO by diffusion NMR, and the quantitative interpretation of the NMR data yielded the number of ligands per nanocrystal, the adsorption isotherm, and the Gibbs free energy of adsorption of TOPO on the InP surface. Capping exchange from TOPO to pyridine was also demonstrated. Apart from the investigation of organic ligands, NMR has also been applied to study the evolution of precursor molecules in the CdSe[20] and PbSe[21] synthesis. The results demonstrated that the ligands not only mediate the reaction speed through steric hindrance but also play an active role during the formation of CdSe and PbSe monomers. NMR can therefore also provide a deeper insight into the mechanisms of the nanocrystal synthesis.

In this study, we have combined nuclear magnetic resonance spectroscopy with inductively coupled plasma mass spectrometry (ICP-MS) to identify and quantify the composition of the organic/inorganic interface of colloidal PbSe nanocrystals, prepared with the Murray synthesis. While every molecule entering the reaction mixture has already been proposed as a possible ligand,[22,23] we found that the Q-PbSe are capped almost exclusively by oleic acid (OA) ligands. The ICP-MS analysis shows that the Q-PbSe contain more lead than selenium, a difference that can be interpreted as a lead surface excess. The combination of the NMR and ICP-MS experimental data with detailed structural modeling of the nanocrystals showed that the number of OA ligands matches the number of excess Pb atoms. The evolution of a Q-PbSe suspension, stored under ambient conditions, was also investigated. The results suggest that oxidation of the Q-PbSe surface is accompanied by a loss of OA ligands and surface Pb atoms, leading to the formation of $Pb(OA)_2$ in solution.

2. Experimental Section

2.1. Materials. Lead acetate trihydrate (99.999%), dibromomethane (99+%, CH_2Br_2), and technical oleic acid (90%) were purchased from Sigma-Aldrich. Higher purity oleic acid (98%) was purchased from Fluka. Selenium powder (−200 mesh, 99.999%) was ordered from Alfa-Aesar. Tri-*n*-octylphosphine (97%) was obtained from Strem Chemicals. Diphenyl ether, methanol, butanol, and toluene were all of quality "for synthesis" and were ordered from VWR. Deuterated toluene (99.96% deuterated, toluene-d_8) was purchased from CortecNet (Eurisotop).

2.2. Q-PbSe Synthesis and Characterization. Monodisperse colloidal PbSe nanocrystal suspensions with a mean size varying between 3 and 7 nm were synthesized using an optimized version of the Murray synthesis,[1] as described in detail in ref 24. Both technical- and high-purity OA were used for the synthesis and yield Q-PbSe suspensions with comparable properties.

The Q-PbSe size and concentration were determined from the absorbance spectrum of a Q-PbSe suspension. The nanocrystal size, d, is given by the band gap, E_0 (the first exciton peak), through a sizing curve, and the nanocrystal concentration, C, was given by the absorption coefficient of the Q-PbSe suspension at 400 nm (A_{400}) through the molar extinction coefficient, ε. Details of the procedure to determine the sizing curve and molar extinction coefficient are given elsewhere.[24]

2.3. Ligand Identification and Quantification. NMR samples were prepared by drying a known amount of Q-PbSe in toluene under a strong nitrogen flow, followed by redispersing the nanocrystals in toluene-d_8. First, the identity of the ligands was established by means of proton (^{1}H) spectra, correlation spectroscopy (COSY), proton−carbon heteronuclear single quantum correlation spectroscopy (^{1}H−^{13}C HSQC), and diffusion ordered spectroscopy (DOSY)[25] measurements.[18] All NMR measurements were performed with a Bruker DRX 500 equipped with a TXI Z-gradient probe and operating at ^{1}H and ^{13}C frequencies of 500.13 and 125.76 MHz respectively. ^{31}P NMR spectra were recorded at 121.44 MHz on a Bruker Avance 300 with a BBO probe. All NMR measurements except the DOSY were done with temperature control, set at 295 K. To suppress convection artifacts, DOSY measurements where either performed with the standard bipolar LED pulse sequence at ambient temperature without temperature control or with the convection compensating dstebpgp3s pulse sequence at a controlled temperature of 295 K. For an adequate sampling of the slowest diffusing species, a gradient pulse duration δ of 5 ms and a diffusion delay Δ of 200−250 ms were used. Values this long might pose a problem with regards to T_1 and T_2 relaxation. Δ must be taken smaller than the T_1 relaxation rate, and 2δ must be smaller than the T_2 relaxation rate to maintain a significant signal-to-noise ratio. To ensure that the restrictions for the DOSY measurements were satisfied, T_1 and T_2 measurements were performed on a Q-PbSe suspension using standard pulse sequences.

With DOSY, one can measure diffusion-weighted ^{1}H spectra, selectively filtering out fast diffusing species with a magnetic field gradient. The signal attenuation is given by the Stejskal−Tanner equation:

$$I = I_0 \exp(-(\gamma s_1 \delta G)^2 D(\Delta - s_2\delta - \tau/2)) \quad (1)$$

Here, s_1 and s_2 are shape factors (correcting for the sinusoidal shape of the gradient pulse), γ is the proton gyromagnetic ratio, G is the gradient pulse strength, τ is the time interval separating the bipolar gradient pulses, and D is the diffusion coefficient. D can be converted to a hydrodynamic diameter d_H using the Stokes−Einstein equation:

$$d_H = \frac{k_B T}{3\pi\eta D} \quad (2)$$

After ligand identification, the ligand grafting density was determined by adding a known amount of CH_2Br_2 (2 μL) as a concentration standard to the NMR samples and measuring the proton spectra under conditions of full T_1 relaxation (relaxation delay 45 s). By comparing the area under the ligand resonances to the area under the CH_2Br_2 resonance, the concentration of ligands

(13) Aldana, J.; Wang, Y. A.; Peng, X. G. *J. Am. Chem. Soc.* **2001**, *123*, 8844.
(14) Majetich, S. A.; Carter, A. C.; Belot, J.; McCullough, R. D. *J. Phys. Chem.* **1994**, *98*, 13705.
(15) Sachleben, J. R.; Colvin, V.; Emsley, L.; Wooten, E. W.; Alivisatos, A. P. *J. Phys. Chem. B* **1998**, *102*, 10117.
(16) Ribot, F.; Escax, V.; Roiland, C.; Sanchez, C.; Martins, J. C.; Biesemans, M.; Verbruggen, I.; Willem, R. *Chem. Commun.* **2005**, 1019.
(17) Van Lokeren, L.; Maheut, G.; Ribot, F.; Escax, V; Verbruggen, I.; Sanchez, C.; Martins, J. C.; Biesemans, M.; Willem, R. *Chem. Eur. J.* **2007**, *13*, 6957.
(18) Hens, Z.; Moreels, I.; Martins, J. C. *ChemPhysChem* **2005**, *6*, 2578.
(19) Moreels, I.; Martins, J. C.; Hens, Z. *ChemPhysChem* **2006**, *7*, 1028.
(20) Liu, H. T.; Owen, J. S.; Alivisatos, A. P. *J. Am. Chem. Soc.* **2007**, *129*, 305.
(21) Steckel, J. S.; Yen, B. K. H.; Oertel, D. C.; Bawendi, M. G. *J. Am. Chem. Soc.* **2006**, *128*, 13032.
(22) Lu, W. G.; Fang, J. Y.; Ding, Y.; Wang, Z. L. *J. Phys. Chem. B* **2005**, *109*, 19219.
(23) Olsson, Y. K.; Chen, G.; Rapaport, R.; Fuchs, D. T.; Sundar, V. C.; Steckel, J. S.; Bawendi, M. G.; Aharoni, A.; Banin, U. *Appl. Phys. Lett.* **2004**, *85*, 4469.
(24) Moreels, I.; Lambert, K.; De Muynck, D.; Vanhaecke, F.; Poelman, D.; Martins, J. C.; Allan, G.; Hens, Z. *Chem. Mater.* **2007**, *19*, 6101.
(25) Wu, D. H.; Chen, A. D.; Johnson, C. S. *J. Magn. Reson., Ser. A* **1995**, *115*, 260.

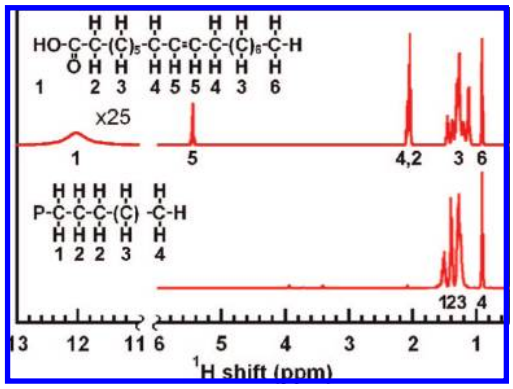

Figure 1. ^{1}H NMR spectra of OA (top) and TOP (bottom) dissolved in toluene-d_8. The methyl and methylene resonances of both molecules partly overlap in the aliphatic region. OA can be distinguished from TOP by its 5.46 ppm resonance corresponding to the olefinic protons. At 12.03 ppm, the carboxylic proton resonance of OA can be observed.

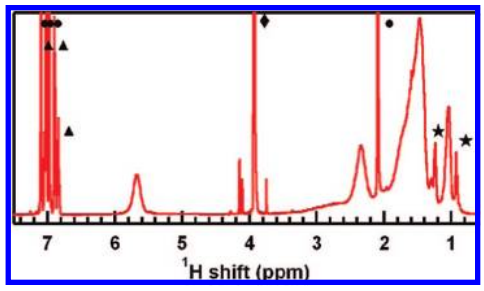

Figure 2. ^{1}H NMR spectrum of a Q-PbSe suspension. Several broad resonances are observed, with a chemical shift comparable to the chemical shift of OA. The sharp resonances can be attributed to toluene-d_8 (●), DPE (▲), CH_2Br_2 (♦), and TOPSe (★).

was determined. From the known concentration of Q-PbSe in the NMR sample, we then derived the number of ligands per nanocrystal.

3. Results and Discussion

3.1. Ligand Identification. The Murray synthesis is based on the formation of PbSe nanocrystals from TOPSe and $Pb(OA)_2$, in presence of an excess of TOP and OA and under inert conditions. This yields TOP and OA as the most likely ligands. Their ^{1}H NMR spectrum in toluene-d_8 is shown in Figure 1. The resonances were assigned using ^{1}H spectra, COSY, and ^{1}H−^{13}C HSQC. The methyl and methylene resonances of TOP all show up in the aliphatic region of the ^{1}H spectrum (1−2 ppm), and there is a strong overlap with the methyl and methylene resonances of OA. Still, OA can be distinguished from TOP by the resonances at 5.46 and 12.03 ppm, corresponding to the olefinic protons and the carboxylic proton, respectively.

A typical ^{1}H NMR spectrum of the Q-PbSe, suspended in toluene-d_8, is shown in Figure 2. Several broad resonances are observed, with chemical shifts comparable to those of OA. Apart from these broad resonances, four other molecules displaying sharp resonances were identified in the Q-PbSe suspension: toluene-d_8 (●); some residual diphenyl ether (DPE, ●); dibromomethane (CH_2Br_2, ♦), added as a concentration standard; and TOPSe (★). As we could not distinguish TOP from TOPSe in the ^{1}H NMR spectrum, the attribution of these signals (★) was based on ^{31}P NMR. ^{31}P measurements on pure TOPSe and pure TOP respectively showed a resonance at 35 and −32 ppm. The

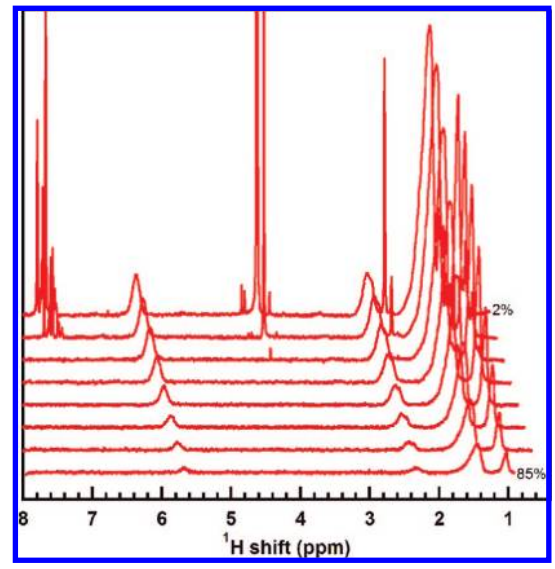

Figure 3. Series of diffusion-filtered spectra (offset for clarity). The gradient strength G varies from 2% to 85% of the maximum value of 56.3 G/cm. At high gradient strength, only the broad resonances persist. The 2.68, 2.05, and 1.75 ppm resonances are not observable in a diffusion-filtered spectrum due to a fast T_2 relaxation.

Table 1. T_1 and T_2 Relaxation Times of the Broad Resonances in the ^{1}H NMR Spectrum of a Q-PbSe Suspension

shift (ppm)	T_1 (s)	T_2 (ms)
5.67	1.00	44.8
2.68	0.68	*a*
2.33	0.68	45.0
2.05	0.69	25.0
1.75	0.66	26.9
1.45	1.04	183
1.07	1.86	337

[a] The T_2 relaxation time of the 2.68 ppm resonance was too short to be measured.

^{31}P spectrum of the Q-PbSe suspension showed a single resonance at 35 ppm, which was consequently assigned to TOPSe.

The attribution of the broad resonances to surface-bound ligands was firmly established using diffusion-ordered NMR spectroscopy (DOSY). Figure 3 shows a series of diffusion filtered spectra of a Q-PbSe suspension, measured with a diffusion delay $\Delta = 200$ ms, a gradient pulse duration $\delta = 5$ ms, and a gradient strength G varying from 2% to 85% of the maximum gradient strength (56.3 G/cm). While the resonances of toluene-d_8, CH_2Br_2, TOPSe, and DPE disappear completely when G reaches 30%, the broad resonances remain clearly visible up to a gradient strength of 85%. This already indicates that they arise from a slowly diffusing species, i.e. the ligands attached to the PbSe nanocrystal surface. One can also see that the broad resonances around 2.68, 2.05, and 1.75 ppm do not show up in the diffusion-filtered spectrum, due to their short T_2 relaxation times (Table 1).

When measuring the signal attenuation as a function of G at fixed Δ and δ, the diffusion coefficient of all resonances observed in the ^{1}H spectrum of the Q-PbSe suspension can be obtained from the Stejskal−Tanner equation. For a typical Q-PbSe suspension, five markedly different diffusion coefficients can be distinguished (Figure 4a, Table 2). Toluene-d_8, DPE, CH_2Br_2, and TOPSe all have relatively fast diffusion coefficients. In contrast, the broad resonances show up with a

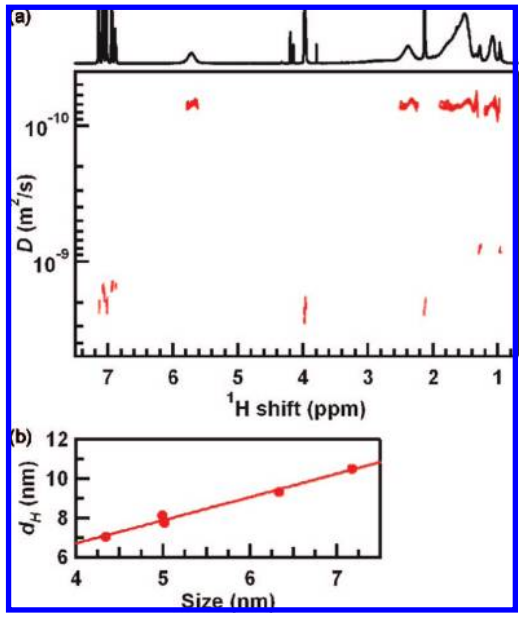

Figure 4. (a) DOSY spectrum of a Q-PbSe suspension. The species associated with the broad resonances diffuses with a diffusion coefficient of 6.96×10^{-11} m^2/s. (b) Plot of the hydrodynamic radius d_H of Q-PbSe nanocrystals in toluene-d_8 versus nanocrystal core size.

Table 2. Chemical Shifts and Diffusion Coefficients (D) for Toluene-d_8, DPE, CH_2Br_2, TOPSe, and the Broad Resonances

	^{1}H shift (ppm)	D (10^{-10} m^2/s)
toluene-d_8	6.9−7.1, 2.09	21.3
DPE	6.8−7.0	15.2
CH_2Br_2	3.98	26.1
TOPSe	0.9−1.4	7.95
broad	5.67, 1.0−2.6	0.696

diffusion coefficient of only 6.96×10^{-11} m^2/s. This corresponds to a hydrodynamic diameter $d_H = 10.5$ nm, which agrees well with the size of the Q-PbSe core (7.2 nm), incremented with the typical thickness of an organic capping layer (1−2 nm). When performing DOSY measurements for differently sized PbSe nanocrystals, we found a clear correlation between the hydrodynamic diameter, calculated from the diffusion coefficient, and the size of the Q-PbSe core (Figure 4b). These results have two important implications. First, the slow diffusion coefficient and excellent correlation between the hydrodynamic diameter and nanocrystal core size show unambiguously that the broad resonances come from the nanocrystal ligands. Second, these ligands are tightly bound to the nanocrystal surface, in a sense that they do not exchange between a bound and an unbound state on the time scale of the DOSY measurement (equal to $\Delta = 200$ ms). This behavior would reveal itself by a larger diffusion coefficient, corresponding to the weighted sum of the diffusion coefficient of the free state and the bound state, respectively.

As already mentioned, the ^{1}H NMR spectrum of a Q-PbSe suspension suggests that the broad resonances can be associated with oleic acid ligands. Further proof follows from a comparison of the ^{1}H−^{13}C HSQC spectra of both OA and a Q-PbSe suspension (Figure 5). One sees that the Q-PbSe HSQC cross peaks indeed agree well with those of OA. The ^{13}C chemical shift of all resonances is comparable for both spectra, while the ^{1}H chemical shift is slightly shifted to lower ppm values in the case of OA. These measurements finally confirm that the broad resonances observed can be attributed to OA ligands.

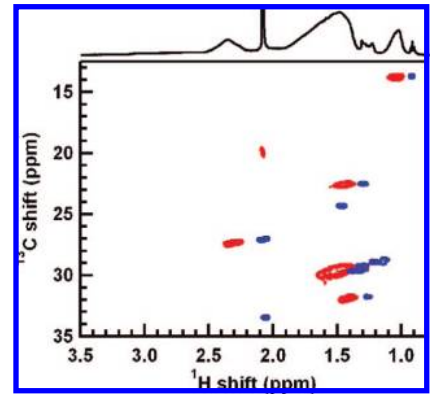

Figure 5. HSQC spectra of OA (blue) and a Q-PbSe suspension (red). Both spectra are well-correlated, confirming that the broad resonances correspond to OA ligands. The 2.68 and 2.05 ppm resonances can no longer be observed, again due to their fast relaxation.

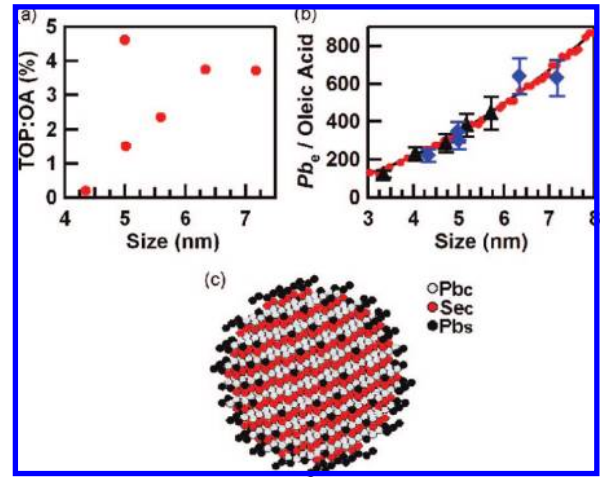

Figure 6. (a) The TOP:OA ligand ratio does not exceed 0.05 for all samples studied. (b) The experimental Pb excess (▲) is well-reproduced by a quasispherical Pb-terminated nanocrystal model (●). It scales with the Q-PbSe surface area, confirming that it is a surface excess. The number of OA ligands per nanocrystal (◆) corresponds well with the Pb excess. (c) Quasispherical Q-PbSe structural model, showing the core Se (red) and Pb (gray) atoms, surrounded by the excess Pb (black) atoms.

Similar to the DOSY measurements, the 2.68 and 2.05 ppm resonances are unobservable in the HSQC spectrum due to their fast relaxation. Unfortunately, this hampers the identification of other potential ligands. As the methyl and methylene resonances of bound OA may overlap with bound TOP, the presence of TOP ligands cannot be excluded or confirmed from the HSQC spectrum alone. We resolved this problem by measuring a ^{1}H NMR spectrum under quantitative conditions. While the 5.46 ppm resonance (with area A_{ol}) can solely be attributed to the olefinic protons of the OA ligands, the resonance at 1.06 ppm (with area A_{Me}) corresponds to the methyl protons of OA and, possibly, TOP. Consequently, the ratio of the respective areas will give the TOP:OA ligand ratio:

$$\text{TOP:OA} = \frac{2A_{ol}/A_{Me} - 3}{9} \qquad (3)$$

Figure 6a shows the TOP:OA ratio for differently sized Q-PbSe. As it does not exceed 0.05, we can conclude that the capping of colloidal PbSe nanocrystals, produced by the Murray synthesis, consists almost exclusively of OA ligands.

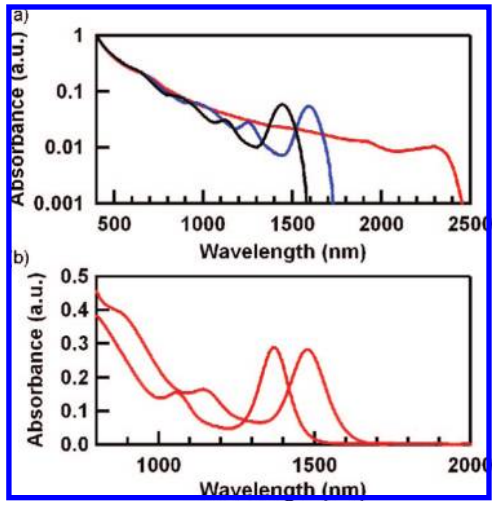

Figure 7. (a) Normalized absorbance spectra of syntheses performed with an OA_e:Pb ratio of 0.65 (red), 1.5 (blue), and 2.4:1 (black). Decreasing the OA_e:Pb ratio leads to larger nanocrystals. (b): The Q-PbSe band gap transition shows a blue shift of 107 nm after storage under ambient conditions for 2 months. This shift corresponds to an effective core size reduction of 0.5 nm, approximately equal to the loss of one monolayer.

Knowing that OA acts as the principle ligand, we hypothesized that it may be essential in terminating the nanocrystal growth during synthesis. We verified this by growing Q-PbSe using different amounts of excess oleic acid (OA_e) (with respect to the Pb precursor). With a 4 min reaction time, and OA_e:Pb ratios of 0.65, 1.5, and 2.4:1, we observed a strong red shift of the Q-PbSe band gap transition with decreasing OA_e:Pb ratio (figure 7a). This result shows that the particle size is very sensitive to the OA_e:Pb ratio. At high ratios, fast termination of the growth keeps the particles small, whereas relatively slow termination leads to large particles at low OA_e:Pb ratios. Figure 7a shows that by decreasing the OA_e:Pb ratio to 0.65:1, 9.5 nm Q-PbSe can be synthesized. Consequently, this approach allows for the one-step synthesis of large (>10 nm) Q-PbSe, avoiding the need to add extra precursors during synthesis.[2]

3.2. Ligand Quantification. When adding 2 μL of CH_2Br_2 to a Q-PbSe suspension as a concentration standard, the number of OA ligands in the suspension can be quantified. From the ratio of the area under the CH_2Br_2 resonance at 3.98 ppm and the area under the olefinic resonance at 5.46 ppm, the OA ligand concentration in the NMR sample was determined. Knowing the Q-PbSe concentration,[24] the number of OA ligands per nanocrystal was calculated (figure 6b). On average, we found a grafting density of 4.2 OA ligands per square nanometer of Q-PbSe surface.

Recently, we reported that PbSe nanocrystals are nonstoichiometric.[24] Determination of the Pb:Se ratio of the nanocrystals with ICP-MS yielded a Pb excess for all samples studied (Q-PbSe sizes ranged from 3 to 6 nm). On the basis of these results, we built a structural model for colloidal PbSe nanocrystals (Figure 6c). It represents the Q-PbSe as faceted spherical nanocrystals, composed of a stoichiometric PbSe core and terminated by a pure Pb surface shell. The theoretical Pb excess (Pb_e) is then defined as the difference between the number of Pb atoms and Se atoms per nanocrystal. Figure 6b shows that the experimental Pb excess (▲) is well-reproduced by the theoretical values (●), validating our Q-PbSe structural model. The results of the quantitative NMR measurements complete our picture of the composition and stoichiometry of the Q-PbSe surface. First, the minor fraction of TOP ligands is consistent with the absence of Se at the Q-PbSe surface. This is in line with the results of Jasieniak and Mulvaney.[26] These authors reported that the luminescence of CdSe nanocrystals with a Cd-rich surface is not affected by the addition of TOP, from which they concluded that TOP does not bind to surface Cd atoms. Second, Figure 6b shows that the number of OA ligands (◆), determined by NMR, matches Pb_e, determined by ICP-MS, almost exactly. On average, we find an OA:Pb_e ratio of 0.97 ± 0.06. This result is quite surprising. It shows that we should not conceive a PbSe nanocrystal as composed of Pb^{2+}, Se^{2-}, and two OA^- ligands per excess lead atom to ensure charge stability. Rather, we should see them as made of Pb, Se, and one OA ligand per excess lead atom. This nonstoichiometric Q-PbSe model clearly has interesting consequences. For instance, recent experimental results have shown that Q-PbSe form linear aggregates in suspension[27] and that PbSe nanowires can be grown through oriented attachment of PbSe nanocrystals.[28] Both results are explained through the existence of a permanent dipole moment. However, as our model is centrosymmetric, the origin of the permanent dipole moment in Q-PbSe is far from obvious, and further research will be needed to bring both results together. From a theoretical viewpoint, the optical properties of colloidal nanocrystals have always been calculated with quasistoichiometric models, using appropriate ligand potentials or pseudohydrogen atoms to passivate surface states.[29,30] We now present a more realistic Q-PbSe model for both the nanocrystal core and the ligand shell, which could improve the comparison between theoretical calculations and experimental results. These calculations could also reveal why Q-PbSe are highly luminescent,[3] in spite of the excess of Pb atoms at the surface.

3.3. Oxidation of a Q-PbSe Suspension. A recent study has shown that the Q-PbSe optical properties are highly sensitive to oxidation.[31] A blue shift of the absorbance and luminescence peaks was observed for samples stored under ambient conditions, corresponding to an effective reduction in size of about 0.3 nm. These results are confirmed by our own measurements. We stored dilute suspensions of Q-PbSe in CCl_4 under ambient conditions for 2 months and observed a blue shift of the absorption peaks for all samples studied. Figure 7b shows a typical absorbance spectrum before and after oxidation. The blue shift (107 nm) corresponds to a decrease in effective diameter of about 0.5 nm, i.e., close to one atomic monolayer.

To understand the mechanism behind the oxidation process, we used NMR to monitor the evolution of a Q-PbSe suspension, stored under ambient conditions. The suspension was prepared under nitrogen, loaded in an NMR tube with a tightly closed screw cap and stored under ambient conditions. At different time intervals after sample preparation, ^{1}H and DOSY spectra were measured (Figure 8).

After 1 week, additional resonances started to appear, at a slightly lower chemical shift than the ligand resonances. DOSY showed that these resonances have a diffusion coefficient of

(26) Jasieniak, J.; Mulvaney, P. *J. Am. Chem. Soc.* **2007**, *129*, 2841.
(27) Klokkenburg, M.; Houtepen, A. J.; Koole, R.; de Folter, J. W. J.; Erne, B. H.; van Faassen, E.; Vanmaekelbergh, D. *Nano Lett.* **2007**, *7*, 2931.
(28) Cho, K. S.; Talapin, D. V.; Gaschler, W.; Murray, C. B. *J. Am. Chem. Soc.* **2005**, *127*, 7140.
(29) An, J. M.; Franceschetti, A.; Dudiy, S. V.; Zunger, A. *Nano Lett.* **2006**, *6*, 2728.
(30) Huang, X. Y.; Lindgren, E.; Chelikowsky, J. R. *Phys. Rev. B* **2005**, *71*, 165328.
(31) Stouwdam, J. W.; Shan, J.; van Veggel, F.; Pattantyus-Abraham, A. G.; Young, J. F.; Raudsepp, M. *J. Phys. Chem. C* **2007**, *111*, 1086.

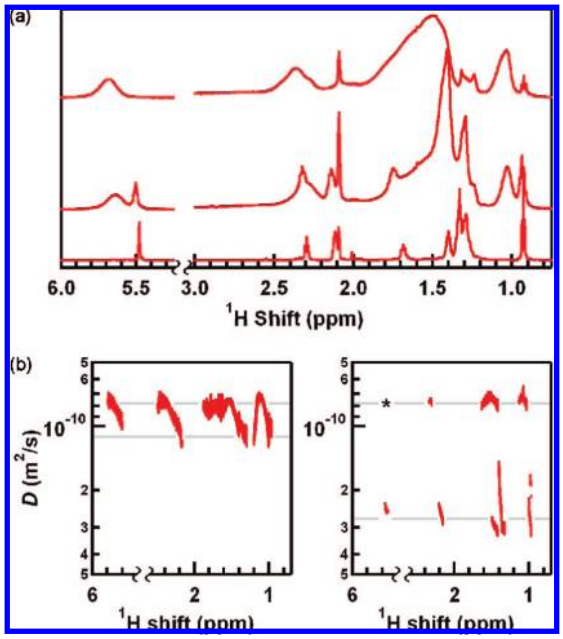

Figure 8. (a) ^{1}H NMR spectra of a fresh Q-PbSe suspension (top), an oxidized Q-PbSe suspension (middle), and a solution of $Pb(OA)_2$ in toluene-d_8 (bottom). After storage under ambient conditions for 1 month, a new set of resonances appears in the ^{1}H spectrum of a Q-PbSe suspension (middle). By comparing this set to the resonances of pure $Pb(OA)_2$ (bottom), we can conclude that the resonances can be attributed to $Pb(OA)_2$. (b) DOSY spectra after 1 week (left) and 1 month (right). The diffusion coefficient of the new set of resonances gradually shifts to higher values as the oxidation progresses, while the diffusion coefficient of the ligand resonances remains at 7.94×10^{-11} m^2/s. This gradual shift suggests a fast chemical equilibrium between adsorbed and free $Pb(OA)_2$. Due to the low signal-to-noise ratio, the diffusion coefficient of the olefinic protons of the Q-PbSe ligands (*) is not included in the right DOSY plot in order to avoid a noisy representation of data.

1.07×10^{-10} m^2/s, which is 35% larger than the diffusion coefficient of the Q-PbSe. Over 1 month, these resonances gradually increase in intensity, and the associated diffusion coefficient increases to 2.85×10^{-10} m^2/s (Figure 8b). Since Q-PbSe suspensions prepared under ambient conditions and loaded in an NMR tube with an ordinary cap show the same evolution in a matter of days, we conclude that these trends reflect the oxidation of the Q-PbSe sample, albeit at a slower pace in the case of the screw cap due to the reduced inflow of oxygen.

In Figure 8a, we also show the ^{1}H spectrum of pure $Pb(OA)_2$. The major difference with the spectrum of OA (Figure 1) is the chemical shift of the protons closest to the carboxylic head groups, equaling 2.29 ppm instead of 2.05 ppm. In the oxidized Q-PbSe spectrum, these protons show a resonance at a chemical shift of 2.32 ppm, a value close to that of $Pb(OA)_2$. This suggests that oxidation leads to the loss of ligands and Pb atoms from the nanocrystal surface, which could explain the observed size reduction of oxidized Q-PbSe. Quantitatively, about 30% of the ligands are released from the nanocrystal surface after 1 month.

Looking at the DOSY spectrum in more detail, we find that the diffusion coefficient of the $Pb(OA)_2$ resonances in the oxidized Q-PbSe suspension is smaller than that of a pure $Pb(OA)_2$ solution in toluene-d_8 (5.00×10^{-10} m^2/s). Moreover, as the $Pb(OA)_2$ resonances increase in intensity over time, their diffusion coefficient also increases slowly. After 1 month, it reaches a value that is 1.8 times smaller than the diffusion coefficient of pure $Pb(OA)_2$. These observations point toward a chemical equilibrium between adsorbed and free $Pb(OA)_2$, with an exchange rate between both states that is fast on the DOSY time scale ($\gg 5$ s^{-1}). In this case, the measured diffusion coefficient D_{eff} equals the weighted sum of the diffusion coefficient of adsorbed (D_{ads}) and free (D_{fr}) $Pb(OA)_2$,

$$D_{eff} = (1 - x)D_{ads} + xD_{fr} \quad (4)$$

where x is the fraction of time the exchanging ligand spends in its free state, and D_{ads} is the diffusion coefficient of the nanocrystals. The increase in measured diffusion coefficient shows that the generated $Pb(OA)_2$ spends more time free in suspension as the surface oxidation progresses, amounting to 46% of the time after 1 month.

4. Conclusions

Using the Murray synthesis, we produced spherical colloidal PbSe nanocrystals of uniform size, with a diameter ranging from 3 to 7 nm. We applied a range of NMR techniques to identify the nanocrystal ligands using solution nuclear magnetic resonance spectroscopy. With a combination of DOSY, HSQC, and quantitative ^{1}H NMR spectra, we could unambiguously determine the composition of the organic capping layer. The PbSe nanocrystals are passivated by OA ligands, with a small amount (0−5%) of TOP also acting as a capping agent. DPE was not detected at the nanocrystal surface, confirming its role as a noncoordinating solvent during synthesis. Because OA acts as an efficient ligand, the Q-PbSe size could be tuned by varying the concentration of OA during synthesis. The number of OA ligands was quantified by adding 2 μL of dibromomethane to the nanocrystal suspension as a concentration standard. We found a grafting density of 4.2 OA ligands per square nanometer of Q-PbSe surface. By combining the NMR results with the results obtained with ICP-MS, we were able to construct a complete structural model of the PbSe nanocrystals. The Q-PbSe are composed of a stoichiometric PbSe core which is terminated by a Pb surface shell. The OA ligands are strongly bound to the surface Pb atoms, at a ratio of one OA ligand for two surface Pb atoms (i.e., for one excess Pb atom). The Q-PbSe are easily oxidized when exposed to air, resulting in an effective core size reduction of about one atomic monolayer (0.5 nm). Due to the oxidation, part of the surface Pb atoms are released from the nanocrystal surface together with the OA ligands, most probably forming $Pb(OA)_2$ in solution. We found that this does not result in a permanent loss of ligands; the new species is rather in an equilibrium state between free and adsorbed $Pb(OA)_2$.

The ICP-MS and NMR measurements are performed, in this case, on colloidal PbSe nanocrystals. The methods and techniques presented here are however extendable to a diverse range of colloidal nanocrystals, especially shape-controlled particles, which are typically synthesized using a mixture of different ligands.[10] In this respect, through the direct observation of the organic ligands with (diffusion) NMR, we believe that new insights can be obtained on the intimate interactions between the nanocrystal core and organic ligand shell during and after synthesis.

Acknowledgment. We acknowledge the Institute for the Promotion of Innovation through Science and Technology in Flanders (IWT-Vlaanderen) for a scholarship (I.M.), the Belgian Science Policy for a research grant (Z.H., IAP 6.10 photonics@be), and the Fund for Scientific Research Flanders (FWO-Vlaanderen) for a research grant (J.C.M., G.0064.07) and an instrument grant (J.C.M., G.00365.03).

JA803994M